Analysis of RC beams subjected to shock loading using a modified fibre element formulation

Hamid R. Valipour[†], Luan Huynh[‡] and Stephen J. Foster[‡†]

Centre for Infrastructure Engineering and Safety(CIES),
School of Civil and Environmental Engineering, The University of New South Wales,
Sydney 2052, Australia

Abstract. In this paper an improved one-dimensional frame element for modelling of reinforced concrete beams and columns subjected to impact is presented. The model is developed in the framework of a flexibility fibre element formulation that ignores the shear effect at material level. However, a simple shear cap is introduced at section level to take account of possible shear failure. The effect of strain rate at the fibre level is taken into account by using the dynamic increase factor (DIF) concept for steel and concrete. The capability of the formulation for estimating the element response history is demonstrated by some numerical examples and it is shown that the developed 1D element has the potential to be used for dynamic analysis of large framed structures subjected to impact of air blast and rigid objects.

Keywords: beam element; flexibility formulation; impact; strain rate; reinforced concrete.

1. Introduction

Research on behaviour of reinforced concrete elements (structures) subjected to high strain rate loading such as impact of dropping mass and air blast have received considerable attention in recent years (Banthia *et al.* 1989, Shirai *et al.* 1994, Kishi *et al.* 2002). The response of beams under impact load has been studied widely by plane and solid elements (Beshara 1993, Abbas *et al.* 2004, May *et al.* 2006), but less attention has been paid to the value of the 1D discrete frame elements for evaluating the global response of beams and framed structures (Krauthammer *et al.* 1990). Plane stress and solid element approaches are more accurate but also significantly more time consuming (computationally) in comparison with 1D discrete elements that are the focus of this paper.

Over the last 20 years the superior performance of the flexibility (force-based) approach in the formulation of frame elements, especially for reinforced concrete members has been demonstrated through different studies (Spacone *et al.* 1996, Neuenhofer and Filippou 1997, Monti and Spacone 2000). Most of the researches in this field have been focused on static and cyclic analysis but the capability of flexibility formulation within a dynamic analysis (especially dynamic loads with high strain rate) have not been discussed. Most of the available flexibility-based frame elements are formulated in the fibre element framework. In the classical fibre element approach, the effect of shear tractions on the nonlinear behaviour of the fibres is assumed to be negligible. In such a case a

---

† Ph. D. candidate, Corresponding author, E-mail: H. Valipour@unsw.edu.au
‡ Ph. D. candidate
‡† Professor

uni-axial constitutive law suffices to calculate the stress and stiffness of the fibres. Two options are available to take account of shear effects. The first option is to couple the shear and axial tractions at the material level (Petrangeli *et al*. 1999). In the second, shear forces are coupled with other forces at section level through empirical relationships, while at the material level the axial and shear stresses do not interact (Marini and Spacone 2006). The first approach is more accurate but also more time consuming (computationally) in comparison with the second.

In this study, the flexibility and force interpolation concept is used to formulate the 1D frame element. The section flexibility (stiffness) is calculated by a numerical integration scheme rather than discritising the section to fibres, which improves the formulation efficiency. A uniaxial constitutive law is used for concrete and steel bars and a shear cap at section level is employed to predict the possibility of shear failure. Adopting the dynamic increase factor (DIF) approach, the strain rate effect on the material behaviour is taken into account.

2. Element formulation

2.1. Equilibrium equations

Fig. (1a) shows a 2-node plane frame element *AB* with three degrees of freedom at each node (two translations and one rotation) subjected to distributed load $w(x)$. The incremental equilibrium equation of the configuration *Ax,* shown in Fig. 1b, yields

$$\Delta \mathbf{D}(x) = \mathbf{b}(x)\Delta \mathbf{Q}_A + \Delta \mathbf{D}^*(x) \tag{1}$$

$$\Delta \mathbf{D}^*(x) = \begin{bmatrix} 0 & -\Delta M^*(x) \end{bmatrix}^T \tag{2}$$

$$\mathbf{b}(x) = \begin{bmatrix} -1 & 0 & 0 \\ 0 & x & -1 \end{bmatrix} \tag{3}$$

where $\Delta \mathbf{D}(x) = [\Delta N(x)\ \Delta M(x)]^T$ is the vector of incremental section generalised force, $\mathbf{b}(x)$ is the force interpolation matrix, $\Delta \mathbf{Q}_A = [\Delta Q_1\ \Delta Q_2\ \Delta Q_3]^T$ is the vector of incremental nodal generalised force at end *A* and $\Delta \mathbf{D}^*(x)$ is the section internal force vector due to the distributed load $\Delta w(x)$.
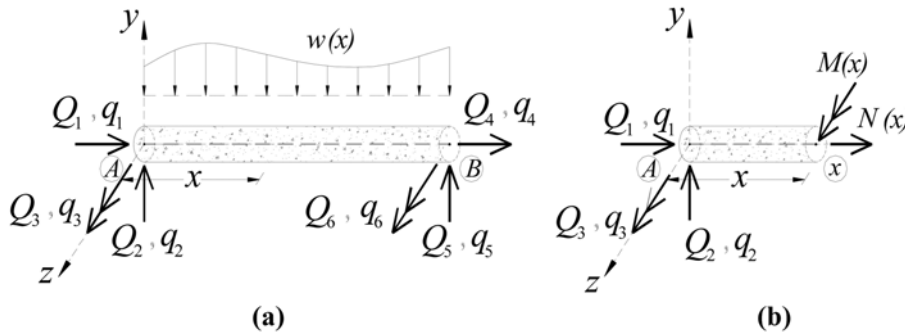

Fig. 1 (a) 2-node frame element *AB* in *x-y* plane (b) free body diagram for *Ax*
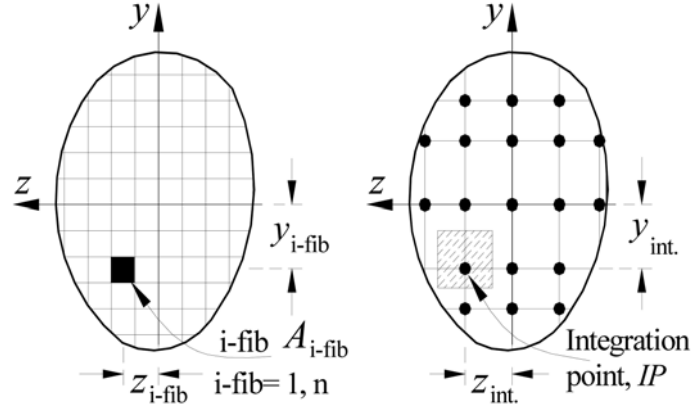
Fig. 2 Comparison of the classical fibre element and present formulation at section level

Removing the term $\Delta \mathbf{D}^{*}(x)$ from the right side of the Eq. (1) does not violate the generality of the formulation and, hence, we can write

$$\Delta \mathbf{D}(x) = \mathbf{b}(x) \, \Delta \mathbf{Q}_A \tag{4}$$

Equilibrium across the section requires that

$$\Delta \mathbf{D}(x) = [\int_{\Omega} \Delta \sigma_x dA - \int_{\Omega} y \Delta \sigma_x dA]^{T} \tag{5}$$

where y is the distance of the integration point from the element mid-plane (see Fig. 2) and $\Delta \sigma_x$ is the increment of the *x-x* stress component at monitoring points.

2.2. Compatibility equations and stress-strain relations

Assuming perfect bond and adopting the Navier-Bernoulli theory, the incremental compatibility requirement is obtained as

$$\Delta \varepsilon_x = \Delta \varepsilon_r - y \Delta \kappa \tag{6}$$

where $\Delta \varepsilon_x$ denotes the increment of the *x-x* strain component at the integration points, $\Delta \varepsilon_r$ denotes the increment of the section axial strain and $\Delta \kappa$ denotes the increment of the section curvature.

Using a uniaxial stress-strain relationship to model the material behaviour at integration points yields

$$\Delta \sigma_x = E_t (\Delta \varepsilon_r - y \Delta \kappa) \tag{7}$$

where E_t is the material tangent modulus.

If Eq. (7) is substituted into Eq. (5), then

$$\Delta \mathbf{D}(x) = {}^{t}\mathbf{k}_s(x) \, \Delta \mathbf{d}(x) = [{}^{t}\mathbf{f}_s(x)]^{-1} \Delta \mathbf{d}(x) \tag{8}$$

$$
{}^{t}k_{s}(x) = \left[{}^{t}\mathbf{f}_{s}(x) \right]^{-1} = \begin{bmatrix} \int_{\Omega} E_{t} dA & -\int_{\Omega} y E_{t} dA \\ -\int_{\Omega} y E_{t} dA & \int_{\Omega} y^{2} E_{t} dA \end{bmatrix} \tag{9}
$$

where ${}^{t}\mathbf{k}_{s}(x)$ and ${}^{t}\mathbf{f}_{s}(x)$ are section stiffness and flexibility matrices, respectively. A network of integration points is provided over the section depth (width) rather than using fibre element method that discritise the section to fibres (Fig. 2). In such a case all of the section integrals can be estimated numerically, which improves the formulation efficiency compared with the classical fibre element.

Using the principle of virtual work for the cantilever configuration *AB*, shown in Fig. 1a, and subjected to a load vector $\Delta\mathbf{Q}_{A}$ at end *A*, together with Eqs. (4) and (8), and then repeating the same procedure for the cantilever clamped at end *A* and subjected to the load vector $\Delta\mathbf{Q}_{B}$ at end *B*, gives the element stiffness matrix ${}^{t}\mathbf{K}_{e}$ as (Valipour and Foster 2007)

$$
{}^{t}\mathbf{K}_{e} = \begin{bmatrix} \left[\int_{0}^{l} \mathbf{b}^{T}(x)\,{}^{t}\mathbf{f}_{s}(x)\mathbf{b}(x)dx \right]^{-1} & \left[\int_{0}^{l} \mathbf{b}^{T}(x)\,{}^{t}\mathbf{f}_{s}(x)\mathbf{b}(x)dx \right]^{-1}\Gamma \\ \Gamma^{T}\left[\int_{0}^{l} \mathbf{b}^{T}(x)\,{}^{t}\mathbf{f}_{s}(x)\mathbf{b}(x)dx \right]^{-1} & \Gamma^{T}\left[\int_{0}^{l} \mathbf{b}^{T}(x)\,{}^{t}\mathbf{f}_{s}(x)\mathbf{b}(x)dx \right]^{-1}\Gamma \end{bmatrix} \tag{10}
$$

where Γ is the transformation matrix

$$
\Gamma = \begin{bmatrix} -1 & 0 & 0 \\ 0 & -1 & L \\ 0 & 0 & -1 \end{bmatrix} \tag{11}
$$

While different solution schemes can be used within the present flexibility formulation, a modified nested iterative algorithm developed by Neuenhofer and Filippou (1997) is adopted in this study.

3. Material constitutive law and strain rate effects

The strength of the concrete and steel bars increase with increasing loading rate. This rate dependent behaviour of material affects the response of the reinforced concrete members under impact and has to be considered by an appropriate method. It is a common practice to use a dynamic increase factor (*DIF*) for transforming the material strength and stress-strain relationship to their dynamic counterpart (Malvar 1998, Malvar and Ross 1999). The *DIF* approach is adopted for taking account of strain rate in this study, even though for materials such as concrete, due to effect of rate history, the adequacy of this approach is questionable in some aspects (Eibl and Schmidt-Hurtienne 1999).

3.1. Concrete constitutive law

Different kinds of concrete material models (e.g., plasticity, continuum damage, micro plane models etc.) with a diverse range of accuracy and generality are available (Chen 1994). In this study the effect of shear on the nonlinear response of material is neglected and the shear failure is

checked at sections. Hence, a uniaxial material law is adequate to model the nonlinear behaviour of concrete.

Among the various available unaxial constitutive laws for plain concrete in compression, the stress-strain law presented by CEB-FIP model code 1990 is adopted for the ascending branch (Fig. 3a),

$$\sigma_c = f_{cp} \frac{k(\varepsilon_c / \varepsilon_{c0}) - (\varepsilon_c / \varepsilon_{c0})^2}{1 + (k-2)(\varepsilon_c / \varepsilon_{c0})}, \quad k = \frac{E_0}{E_c} \tag{12}$$

where f_{cp} and ε_{c0} are the uniaxial concrete compressive strength and corresponding strain, respectively, E_0 is the initial elastic modulus, E_c is the secant elastic modulus at the peak stress and k is a parameter that has a positive value greater than or equal to one. For the sake of simplicity, in conjunction with this ascending relationship a linear softening branch down to the zero stress can be adopted. With regard to the softening branch of the stress-strain relationship and potential for lack of objectivity over softening regime, a regularisation technique similar to crack band model is adopted to preserve the energy release rate and maintain objectivity (Spacone and Coleman 1999). Other methods for maintaining objectivity are presented in Valipour and Foster (2009). The confining effect on the concrete ductility and strength can be modelled by modifying the compressive strength, f_{cp}, the corresponding strain, ε_{c0}, and the compressive ultimate strain, ε_{uc}, according to available uniaxial models (Scott *et al.* 1982, Mander *et al.* 1988).

Unloading from a point on the envelope curve takes place along a straight line connecting the point ε_r, at which unloading starts, to a point ε_p on the strain axis given by the equations (see Fig. 3a)

$$\frac{\varepsilon_p}{\varepsilon_0} = 0.145 \left(\frac{\varepsilon_r}{\varepsilon_0}\right)^2 + 0.13 \left(\frac{\varepsilon_r}{\varepsilon_0}\right), \quad \left(\frac{\varepsilon_r}{\varepsilon_0}\right) < 2$$

$$\frac{\varepsilon_p}{\varepsilon_0} = 0.707 \left(\frac{\varepsilon_r}{\varepsilon_0} - 2\right) + 0.834, \quad \left(\frac{\varepsilon_r}{\varepsilon_0}\right) \geq 2 \tag{13}$$

where ε_0 is the strain corresponding to the peak stress ($\varepsilon_0 \geq \varepsilon_{c0}$ with confinement).

For the tensile concrete a linear elastic brittle failure model is adopted (Fig. 3b). In this model the material follows a linear elastic branch up to tensile strength, f_t, and after that the material fails and cannot carry any stress.
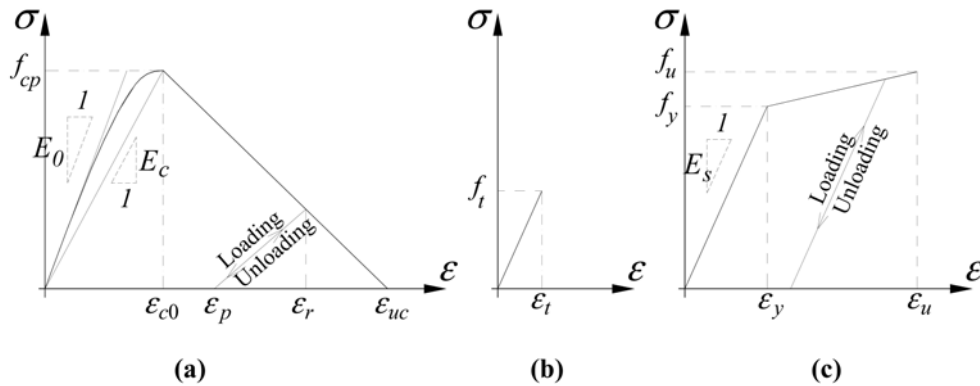

Fig. 3 Stress-strain relationship of (a) concrete in compression, (b) concrete in tension, and (c) reinforcing steel

The DIF_t proposed by Ross *et al.* (1989) is used to take account of the strain rate effect on the concrete tensile strength. For concrete under compression the DIF_c used by Fujikake *et al.* (2000) is adopted. That is,

$$DIF_t = \exp\left[0.00126\left(\log\frac{\dot{\varepsilon}}{\dot{\varepsilon}_{st}}\right)^{3.373}\right] \tag{14}$$

$$DIF_c = \left(\frac{\dot{\varepsilon}}{\dot{\varepsilon}_{sc}}\right)^{0.006\left[Log\left(\frac{\dot{\varepsilon}}{\dot{\varepsilon}_{sc}}\right)\right]^{1.05}} \tag{15}$$

where DIF_t and DIF_c denote the dynamic increase factor for concrete under tension and compression, respectively, $\dot{\varepsilon}$ is strain rate (sec^{-1}), $\dot{\varepsilon}_{sc} = 1.2 \times 10^{-5}$ (sec^{-1}) and $\dot{\varepsilon}_{st} = 1.0 \times 10^{-7}$ (sec^{-1}).

3.2. Steel constitutive law

A bilinear stress-strain relationship with linear unloading is used for steel bars (Fig. 3c). The *DIF* proposed by Malvar (1998) is used to account for the strain rate effect on the yield, f_y, and ultimate strength, f_u, of the reinforcing bars (Malvar 1998). That is

$$DIF_{fy} = \left(\frac{\dot{\varepsilon}}{10^{-4}}\right)^{0.074 - 0.04\left(\frac{f_y}{414}\right)} \tag{16}$$

$$DIF_{fu} = \left(\frac{\dot{\varepsilon}}{10^{-4}}\right)^{0.019 - 0.009\left(\frac{f_y}{414}\right)} \tag{17}$$

These relationships are valid for steels with a yield stress in the rage of $290 \le f_y \le 710$ MPa and for strain rates $10^{-4} \le \dot{\varepsilon} \le 225$ sec^{-1}.

3.3. Shear cap for possible shear failure

In the present formulation a shear cap is used to take account of shear failure at section level. In this study ultimate shear resistance of the sections V_r is taken from ACI-318 (2005) as

$$V_r = 0.17\sqrt{f_{cp}}bd + A_v f_{yh}d/s_h \tag{18}$$

where b is the section width, d is the effective depth of the section, f_{yh} is the yield strength of the transverse reinforcement and A_v and s_h represent the area and spacing of the transverse reinforcement, respectively. As Eq. (18) lacks consideration of the strain rate effect, it is conservative; however, dynamic compressive strength of concrete can be used in Eq. (18) to partly take account of the strain rate effect.

It should be noted that such a simplistic cap model along with Navier-Bernoulli assumption adopted for formulation limits the applicability of the element to cases where the shear deformation and strength do not govern the member response, such as beams with span to depth ratios greater than or equal to five.

4. Dynamic equilibrium equations

The dynamic equilibrium equation of a discritised system in the instant $t+\Delta t$ is

$$\mathbf{M}^{t+\Delta t}\ddot{\mathbf{U}}^{(k)}+\mathbf{C}^{t+\Delta t}\dot{\mathbf{U}}^{(k)}+{}^{t+\Delta t}\mathbf{K}^{(k-1)}\Delta\mathbf{U}^{(k)}={}^{t+\Delta t}\mathbf{R}-{}^{t+\Delta t}\mathbf{F}^{(k-1)} \qquad (19)$$

where $\mathbf{M}$ is the mass matrix, $\mathbf{C}$ is the damping matrix, ${}^{t+\Delta t}\mathbf{K}^{(k-1)}$ is the tangent stiffness matrix with superscript (k) denoting the iteration number, ${}^{t+\Delta t}\mathbf{R}$ is the external load vector, ${}^{t+\Delta t}\mathbf{F}^{(k-1)}$ is internal force vector, $\ddot{\mathbf{U}}$ is the acceleration vector, $\dot{\mathbf{U}}$ is the velocity vector and $\Delta\mathbf{U}^{(k)}$ is the vector of displacement increment.

Using the Newmark implicit integration scheme and substituting the corresponding value of the acceleration and velocity vectors in Eq. (19) leads to the following equations which are solved iteratively:

$$^{t+\Delta t}\hat{\mathbf{K}}^{(k-1)}\Delta\mathbf{U}^{(k)}={}^{t+\Delta t}\Delta\mathbf{R}-{}^{t+\Delta t}\Delta\mathbf{F}^{(k-1)}-\frac{1}{\Delta t}\hat{\mathbf{C}}^{t+\Delta t}\Delta\mathbf{U}^{(k-1)}+\hat{\mathbf{C}}^{t}\dot{\mathbf{U}}+\hat{\mathbf{M}}^{t}\ddot{\mathbf{U}} \qquad (20)$$

$$\hat{\mathbf{K}}=\mathbf{K}+\frac{\delta}{\alpha\Delta t}\mathbf{C}+\frac{1}{\alpha\Delta t^{2}}\mathbf{M} \qquad (21)$$

$$\hat{\mathbf{C}}=\frac{1}{\alpha\Delta t}\mathbf{M}+\frac{\delta}{\alpha}\mathbf{C} \qquad (22)$$

$$\hat{\mathbf{M}}=\frac{1}{2\alpha}\mathbf{M}-\frac{\Delta t}{2}\left(2-\frac{\delta}{\alpha}\right)\mathbf{C} \qquad (23)$$

In Eqs. (21) to (23), α and δ are Newmark integration parameters. In this paper the algorithm proposed by Neuenhofer and Filippou (1997) is employed to calculate ${}^{t+\Delta t}\Delta\mathbf{F}^{(k-1)}$ in Eq. (20) at each stage of the iterative process.

5. Numerical examples

5.1. Beam under impulse concentrated load

A simply supported beam subjected to two concentrated loads applied instantly at mid span is analysed (Bathe and Ramaswamy 1979). The geometry of the beam section, the span and the details are shown in Fig. (4). The material properties are f_{cp}=26 MPa, E_c=42000 MPa, ε_{c0}=0.002, f_t=3.1 MPa, f_y=304 MPa, E_s=206000 MPa, ρ_c=20 kN/m^3 (concrete weight density) and ρ_s=69 kN/m^3 (steel weight density). The applied loads consist of a 60 kN impulse load applied at time t=0 with the load then maintained with increasing time.

One half of the beam was modelled by 3 elements within the flexibility method (Fig. 4). In the flexibility formulation a composite Simpson's integration scheme with 13 integration points through the section depth is used. The distance between longitudinal integration points varies from 90 to 110 mm. The time history of mid span deflection is shown in Fig. (5). In this example, the damping effect was neglected and a Newmark integration technique with α=0.25 and δ=0.5 and maximum time step of 1.0 ms adopted for solving the incremental dynamic equilibrium equations. A lumped mass matrix approach was adopted with a diagonal component scaling. The results are compared
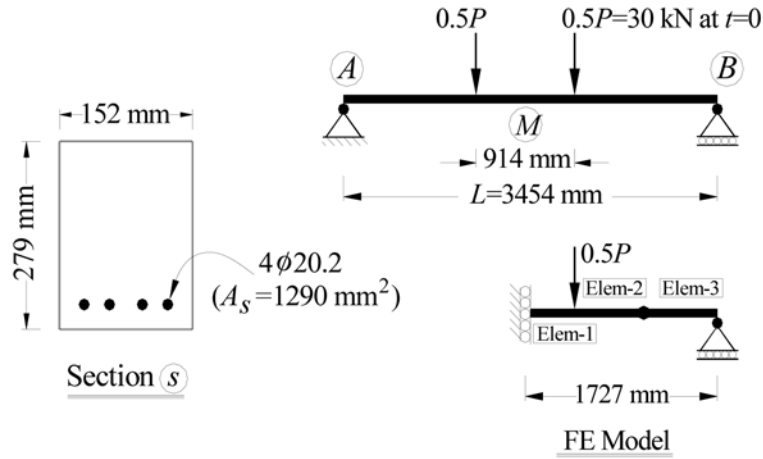
Fig. 4 Geometry of the beam and section details (Bathe and Ramaswamy 1979)

with the 2D displacement based finite element modelling approach of Beshara (1993) and 3D approach of Bathe and Ramaswamy (1979) using the finite element code ADINA. In the ADINA analysis the strain rate effect is not taken into account and for this reason the value of the maximum deflection compared with the results of the present study and with the rate dependent model of Beshara (1993) is overestimated. It is observed that the correlation between the 1D frame element result and the more expensive FE such as plane stress (Beshara 1993) and solid (Bathe and Ramaswamy 1979) models is reasonable.

5.2. Seabold (1967) simply supported beam

In this example a simply supported beam (specimen WE5) tested by Seabold (1967) under the simulated blast pressure is analysed. The geometry of the beam, section detail and pressure-time history is shown in Figs (6) and (7), respectively, the material properties are, f_{cp}=27 MPa, E_c=24000 MPa, ε_{c0}=0.003, f_t=2.7 MPa, f_y=480 MPa, E_s=200000 MPa, ρ_c=21 kN/m^3 and ρ_s=69 kN/m^3.
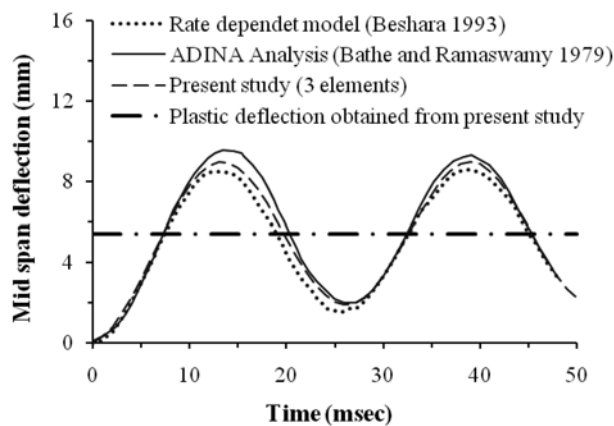

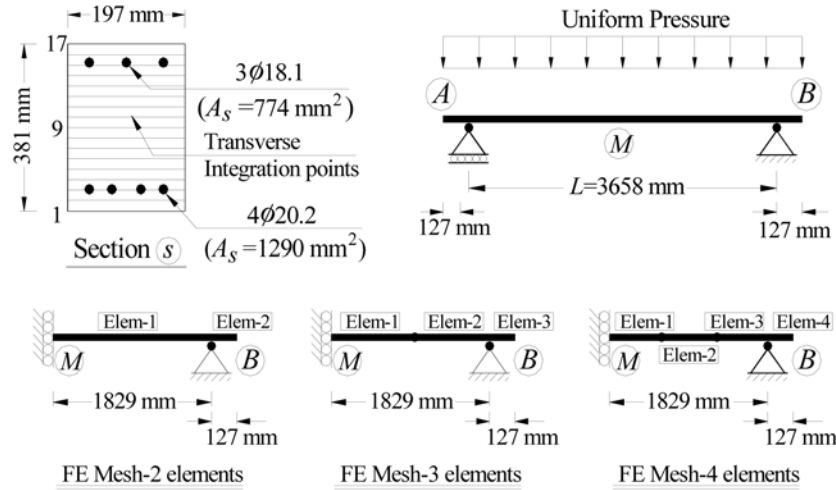Fig. 5 Mid span deflection time history

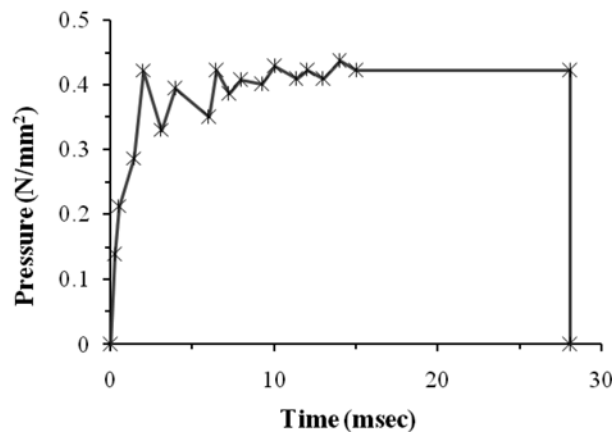Fig. 6 Geometry of the beam and section details (Seabold 1967)

Fig. 7 Pressure time history (Seabold 1967)

One half of the Seabold beam is modelled (including the cantilever) using 2 to 4 elements within the flexibility method (Fig. 6). A composite Simpson's integration scheme was adopted with 17 integration points through the section depth and the distance between longitudinal integration points between 90 and 110 mm. A Newmark integration scheme was used for solving the incremental dynamic equilibrium equations with $\alpha = 0.25$, $\delta = 0.5$ and maximum time step of 0.5 ms. A lumped mass matrix approach was adopted with a diagonal component scaling method used for constructing the matrix. The mid span deflection and velocity history (neglecting damping) are shown in Fig. (8). In Fig (9a) the mid span deflection versus time obtained from the flexibility model is plotted for the different number of elements. It is observed that the response obtained from the model with just 2 elements provides an acceptable accuracy.

The effect of the Rayleigh damping with a mass matrix multiplier of α=0.0005 and initial stiffness matrix multiplier of b=0.01 on the mid span deflection of beam is investigated in Fig. (9b). The permanent deformation of the beam obtained from present study is 18.4 mm, which compares
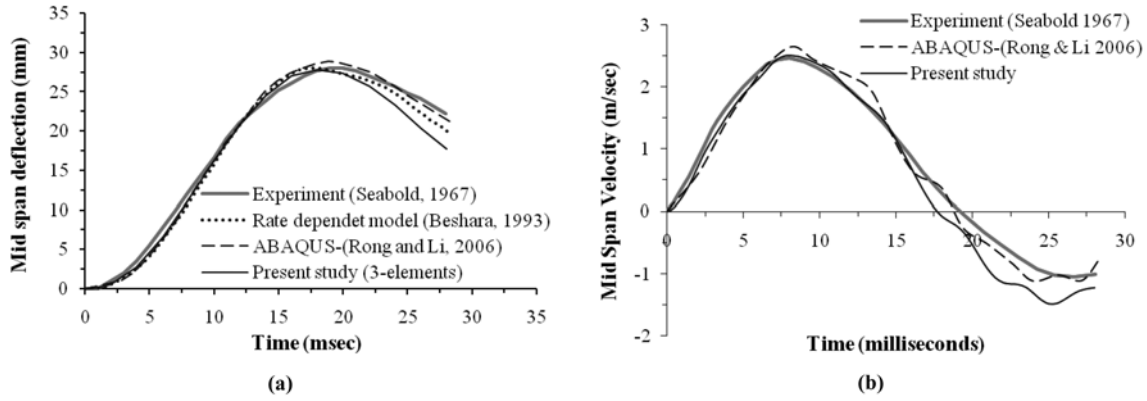
Fig. 8 Comparisons of time versus (a) mid span deflection and (b) mid-span velocity for FE model developed
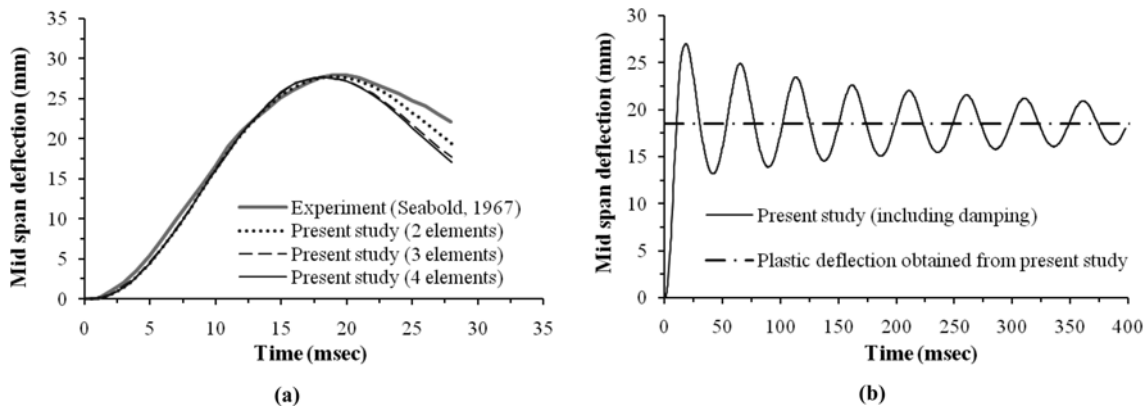with test data and analyses of other investigators

Fig. 9 Time versus mid-span deflection for (a) mesh refinement and (b) free vibration response with damping

favourably with the experimental result of 20.8 mm and 19.7 mm in the analysis of Beshara (1993). The analyses were performed on a Pentium-M notebook computer with a 1.6 GHz processor and running Windows XP. The total analysis time for the model with 3 elements was 0.55 seconds for 60 steps, indicating the efficiency of the method.

5.3. Simple beam subjected to impact of dropping mass

A simply supported beam (specimen SS3a-1) tested by Saatci (2007) and subjected to impact of a dropping mass is analysed. The geometry of the beam, the section details and impact load-time history are shown in Fig. (10). The material properties for the specimen are: f_{cp}=47 MPa, E_c=34000 MPa, ε_{c0}=0.0025, f_t=3.2 MPa, f_y=464 MPa, E_s=195000 MPa, ρ_c=24 kN/m^3 and ρ_s=70 kN/m^3.

One half of the beam was modelled using 5 beam elements (Fig. 10a) with numerical integration through the section depth using a composite Simpson's integration scheme with 21 integration points. The distance between the longitudinal integration points varied from 110 to 130 mm. In this example, the Newmark integration technique with α=0.25 and δ=0.5 and maximum time step of
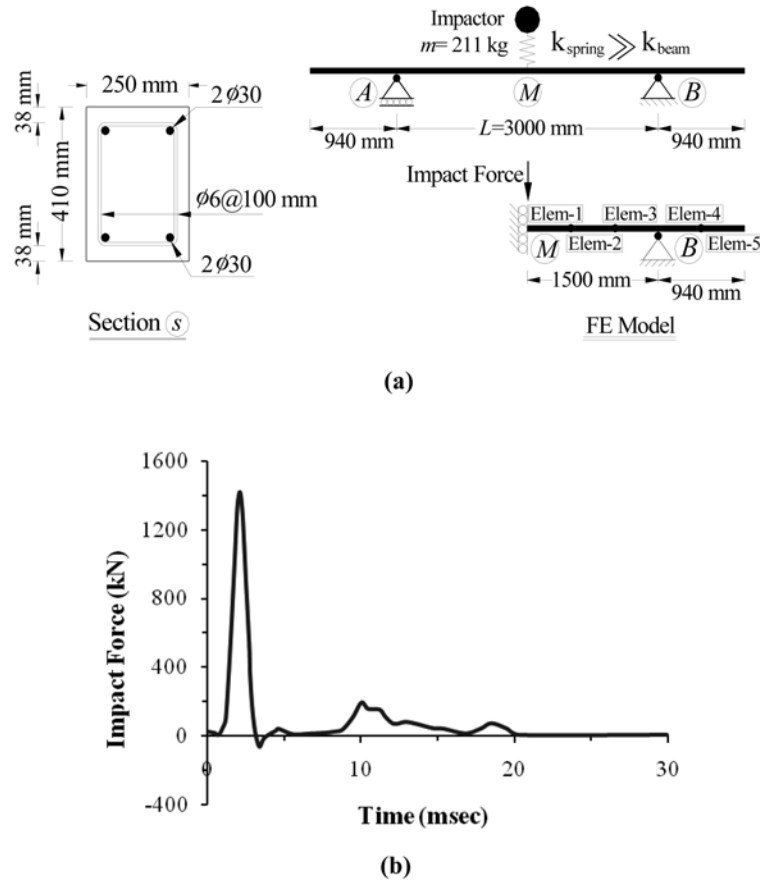
Fig. 10 (a) Geometry of the beam, section details and FE model, and (b) impact force-time history of impact
   test of Saatci (2007)

0.1 ms is used for solving the incremental dynamic equilibrium equations. A lumped mass matrix approach is adopted with a diagonal component scaling method and Rayleigh damping employed with a mass matrix multiplier of $a=0.05$ and initial stiffness matrix multiplier of $b=0.0001$.

Two analyses are undertaken, in the first the time history of the impact force, shown in Fig. (10b), is imposed on the beam. The mid-span deflection versus time and the support reactions versus time obtained from the analysis are shown in Figs. (11a) and (11b), respectively. It is observed that the flexibility model developed here can reasonably predict the displacement and force response of the beam. The total analysis time with 2000 time steps for the model with 5 elements was just 8.70 seconds. This compares with analysis times of more than 2 hours by Saatci and Vecchio (2005) to analyse similar problems using displacement based plane stress finite elements and demonstrates the superior efficiency of the model developed in this paper.

In a second analysis for this example, the mass and velocity of the impactor are input, in lieu of the force-time history. In the literature different approaches with various levels of complexity and accuracy, which mostly inspired from SDOF models, are available to estimate the impact force (Krauthammer *et al*. 1990, Miyamoto *et al*. 1994). In this paper a simple method based on hard impact model of CEB code (1988) is used to verify the applicability of the procedure for cases
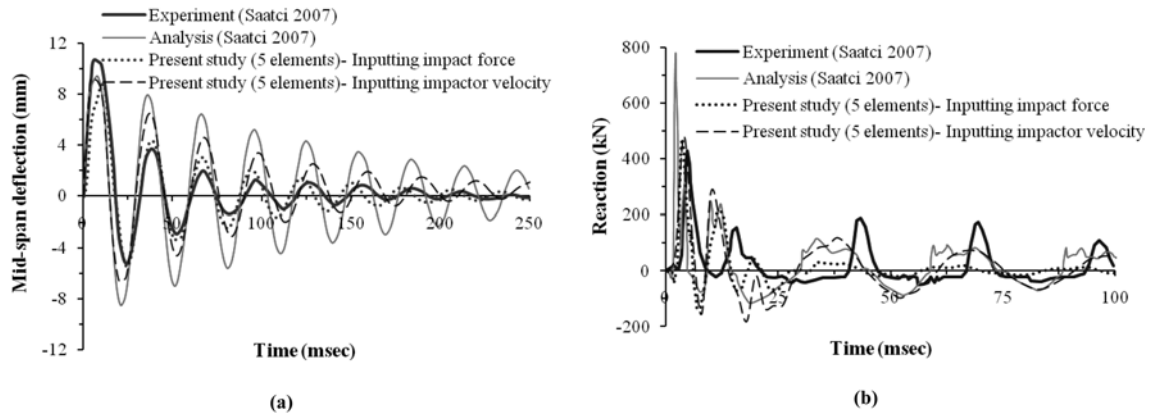
Fig 11 (a) Mid span deflection time history and (b) reaction time history of Saachi (2007) test

inputting impact velocity of the impactor. The mass of the impactor, *m*, is attached to a spring that is just working in compression and this system of mass-spring is attached to the beam mid-span. The impact velocity of the dropping mass (*v*=8.0 m/sec) is imposed to the mass *m* and the ensuing dynamic response is obtained. It is noteworthy that for this example the contact spring was replaced by a rigid truss element that can carry compression only. The results of analysis obtained from this procedure are given in Fig. 11 and shows good correlation with experimental data and leads to a more accurate prediction of support reaction compared with other analytical procedures. It should be noted that the accuracy of results in such a procedure may be sensitive to interface stiffness and impact type (i.e., soft and hard). However, in this example the adopted assumptions have provided reasonably good results.

5.4. Beam subjected to air blast pressure

In this example, beam B140-D2 of Magnusson and Hallgren (2004) subjected to uniform air blast
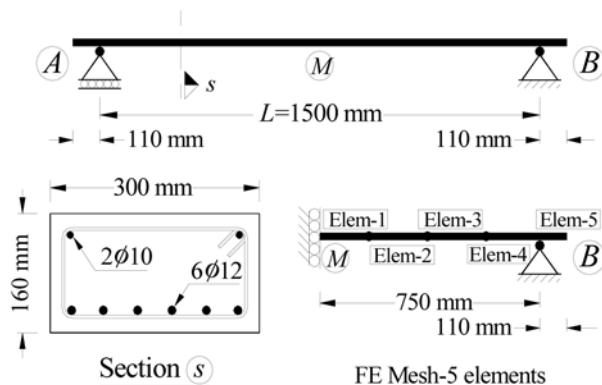

Fig. 12 Geometry of beam and section details for beam B140-D2 of Magnusson and Hallgren (2004) test
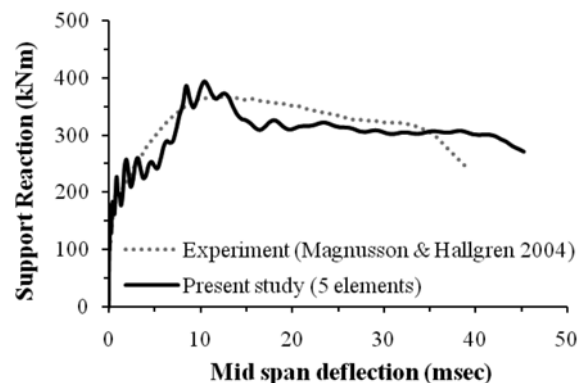
Fig. 13 Mid-span deflection versus support reaction for beam B140-D2 of Magnusson and Hallgren (2004) test

pressure is analysed. The geometry of the beam and details of section is shown in Fig. (12). The average maximum air blast pressure and corresponding impulse density are, p_r=1.55 MPa and i=8.34 kPa and the material properties are: f_{cp}=92 MPa, E_c=45000 MPa, ε_{c0}=0.002, f_t=3.5 MPa, f_y=555 MPa, E_s=200000 MPa, ρ_c=24 kN/m^3 and ρ_s=69 kN/m^3. One half of the beam was modelled using 5 flexibility-based elements (Fig. 12). A composite Simpson's integration scheme with 15 integration points through the section depth was used.

The distance between longitudinal integration points varied from 55 to 70 mm. The damping effect is neglected and a maximum time step of 0.05 ms was adopted for the analysis. The mid span deflection versus support reaction is shown in Fig. (13) with a good correlation observed between analytical model and test data. Furthermore, the failure mode predicted by analytical procedure is of flexural type associate with yielding of steel bars, which is consistent with that recorded in the experiment.

6. Conclusions

The capability of the flexibility formulation for dynamic analysis of reinforced concrete beams subjected to high strain rate loads, such as impact of simulated blast and dropping mass, was investigated. The effect of strain rate on the concrete and on the steel bars strength was taken into account using the dynamic increase factor approach. It is shown that if the dominant failure mode is of a flexural type, the classic fibre element approach accompanied with the flexibility method can offer great efficiencies while maintaining good accuracy. Accordingly, the formulation and analytical tool developed in this paper have a good potential to be used for nonlinear dynamic analysis of reinforced concrete framed structures subjected to the impact of air blast loading.

It was shown that the proposed numerical procedure can incorporate the simplified model based on mass-spring system to calculate the impact force of impacting object as well as the nonlinear response of the structure. In cyclic/static analysis of frames, a single flexibility-based element suffices to capture the nonlinear response of the element and this feature makes the flexibility method superior to displacement-based element approaches. In dynamic analysis of beams subjected to impact, due to the effects of higher modes, the beam should be modelled by a few elements to capture the response reasonably.

References

Abbas, H., Gupta, N.K. and Alam, M. (2004), "Nonlinear response of concrete beams and plates under impact loading", *Int. J. Impact Eng.*, **30**(8-9), 1039-1053.

Banthia, N., Mindess, S., Bentur, A. and Pigeon, M. (1989), "Impact testing of concrete using a drop-weight impact machine", *Exp. Mech.*, **29**(1), 63-69.

Bathe, J.K. and Ramaswamy, S. (1979), "On three-dimensional nonlinear analysis of concrete structures", *Nucl. Eng. Des.*, **52**, 385-409.

Beshara, F.B.A. (1993), "Smeared crack analysis for reinforced concrete structures under blast-type loading", *Eng. Fract. Mech.*, **45**(1), 119-140.

CEB model code: Design code (1988), London, Thomas Telford.

Chen, W.F. (1994), *Constitutive equations for engineering materials,* Amsterdam, Elsevier.

Eibl, J. and Schmidt-Hurtienne, B. (1999), "Strain-rate-sensitive constitutive law for concrete", *J. Eng. Mech.,*

125(12), 1411-1420.

Fujikake, K., Mori, K., Uebayashi, T., Ohno, T. and Mizuno, J. (2000), "Dynamic properties of concrete materials with high rates of tri-axial compressive loads", *Structures Under Shock and Impact VI,(Eds. Jones, N. and Brebbra, C.A.)*, WIT press, 511-522.

Kishi, N., Mikami, H., Matsuoka, K.G. and Ando, T. (2002), "Impact behavior of shear-failure-type RC beams without shear rebar", *Int. J. Impact Eng.*, **27**(9), 955-968.

Krauthammer, T., Shahriar, S. and Shanaa, H.M. (1990), "Response of reinforced concrete elements to severe impulsive loads", *J. Struct. Eng.*, **116**(4), 1061-1079.

Magnusson, J. and Hallgren, M. (2004), "Reinforced high strength concrete beams subjected to air blast loading", WIT Press, Southampton, SO40 7AA, United Kingdom, 53-62.

Malvar, L.J. (1998), "Review of static and dynamic properties of steel reinforcing bars", *ACI Mater. J.*, **95**(5), 609-616.

Malvar, L.J. and Ross, C.A. (1999), "Review of strain rate effects for concrete in tension", *ACI Mater. J.*, **96**(5), 614-616.

Mander, J.B., Priestley, M.J.N. and Park, R. (1988), "Theoretical stress-strain model for confined concrete", *J. Struct. Eng.*, **114**(8), 1804-1826.

Marini, A. and Spacone, E. (2006), "Analysis of reinforced concrete elements including shear effects", *ACI Struct. J.*, **103**(5), 645-655.

May, I.M., Chen, Y., Roger, D., Owen, J., Feng, Y.T. and Thiele, P.J. (2006), "Reinforced concrete beams under drop-weight impact loads", *Comput. Concrete*, **3**(2-3), 79-90.

Miyamoto, A., King, M.W. and Fujii, M. (1994), "Integrated analytical procedure for concreteslabs under impact loads", *J. Struct. Eng-ASCE*, **120**(6), 1695-1702.

Monti, G. and Spacone, E. (2000), "Reinforced concrete fibre beam element with bond-slip", *J. Struct. Eng.*, **126**(6), 654-661.

Neuenhofer, A. and Filippou, F.C. (1997), "Evaluation of nonlinear frame finite-element models", *J. Struct. Eng.*, **123**(7), 958-966.

Petrangeli, M., Pinto, P.E. and Ciampi, V. (1999), "Fibre element for cyclic bending and shear of RC structures. I: theory", *J. Eng. Mech.*, **125**(9), 994-1001.

Ross, C.A., Thompson, P.Y. and Tedesco, J.W. (1989), "Split-hopkinson pressure-bar tests on concrete and mortar in tension and compression", *ACI Mater., J.* **86**(5), 475-481.

Saatci, S. (2007), *Behaviour and modelling of reinforced concrete structures subjected to impact loads*, PhD Dissertation, University of Toronto, Toronto.

Saatci, S. and Vecchio, F.J. (2005), "Finite element analysis of shear-critical reinforced concrete beams under impact loading", *Proceedings of the 6th ASIA-PACIFIC Conference on Shock and Impact Loads on Structures*, Perth, December.

Scott, B.D., Park, R. and Priestley, M.J.N. (1982), "Stress-strain behaviour of concrete confined by overlapping hoops at low and high strain rates", *J. Proceed.*, **79**(1), 13-27.

Seabold, R.H. (1967), "Dynamic shear strength of reinforced concrete beams, Part 2", AD0644823, Technical rept., Jan 65-Jun 66.

Shirai, K., Ito, C. and Onuma, H. (1994), "Numerical studies of impact on reinforced concrete beam of hard missile", *Nucl. Eng. Des.*, **150**(2-3), 483-489.

Spacone, E. and Coleman, J. (1999), "Localization issues in nonlinear frame analysis", *Structures Congress - Proceedings*, 418-421.

Spacone, E., Filippou, F.C. and Taucer, F.F. (1996), "Fibre beam-column model for non-linear analysis of R/C frames: Part I. Formulation", *Earthq. Eng. Struct. D.*, **25**(7), 711-725.

Valipour, H.R. and Foster, S.J. (2007), "A Novel flexibility based beam-column element for nonlinear analysis of reinforced concrete frames", *Report No. Unciv R-447*, University of New South Wales, Sydney.

Valipour, H.R. and Foster, S.J. (2009), "Non-local damage formulation for a flexibility-based frame element", *J. Struct. Eng-ASCE*, (posted online 1 April 2009 doi:10.1061/(ASCE)ST.1943-541X.0000054).

CC